Accepted by the faculty of the Department of Physics and Astronomy, James Madison University, in partial fulfillment of the requirements for the Degree of Bachelor of Science.

FACULTY COMMITTEE:

Dr. Anca Constantin
Associate Professor, Department of Physics and Astronomy

Dr. Harold Butner
Associate Professor, Department of Physics and Astronomy

Dr. Keigo Fukumura
Assistant Professor, Department of Physics and Astronomy

Dr. Bradley Newcomer
Honors Committee Chair

Mid-IR Properties of H_2O Megamaser Disks

A Project

Presented to

the faculty of the Undergraduate College of

Science and Mathematics

James Madison University

In Partial Fulfillment

of the Requirements for the Degree

Bachelor of Science

---

by

C. A. Witherspoon

2017

Contents

List of Tables

List of Figures

Acknowledgments

This thesis would not have been possible without the help of my thesis advisor, Dr. Anca Constantin. I would also like to thank my readers for this thesis: Dr. Keigo Fukumura and Dr. Harold Butner. I acknowledge very helpful discussions and help on *WISE* and SDSS data mining from JMU undergraduates James Corcoran and Emil Christensen. This research was funded in part by 4-VA, a collaborative partnership for advancing the Commonwealth of Virginia.

I am grateful to Jim Braatz for allowing us to use the MCP catalog compilation of the galaxy sample surveyed for water maser emission before publication.

This research has also made use of NASA's Astrophysics Data System and of the NASA/IPAC Extragalactic Database (NED) which is operated by the Jet Propulsion Laboratory, California Institute of Technology, under contract with the National Aeronautics and Space Administration.

This honors thesis has made use of data products from the *Wide-field Infrared Survey Explorer* (*WISE*) and the SDSS.

WISE is a joint project of the University of California, Los Angeles, and the Jet Propulsion Laboratory/California Institute of Technology, funded by the National Aeronautics and Space Administration.

SDSS is managed by the Astrophysical Research Consortium for the Participating Institutions of the SDSS-III Collaboration including the University of Arizona, the Brazilian Participation Group, Brookhaven National Laboratory, Carnegie Mellon University, University of Florida, the French Participation Group, the German

Participation Group, Harvard University, the Instituto de Astrofisica de Canarias, the Michigan State/Notre Dame/JINA Participation Group, Johns Hopkins University, Lawrence Berkeley National Laboratory, Max Planck Institute for Astrophysics, Max Planck Institute for Extraterrestrial Physics, New Mexico State University, New York University, Ohio State University, Pennsylvania State University, University of Portsmouth, Princeton University, the Spanish Participation Group, University of Tokyo, University of Utah, Vanderbilt University, University of Virginia, University of Washington, and Yale University. This research has made use of the NASA/IPAC Extragalactic Database (NED) which is operated by the Jet Propulsion Laboratory, California Institute of Technology, under contract with the National Aeronautics and Space Administration. Funding for SDSS has been provided by the Alfred P. Sloan Foundation, the Participating Institutions, the National Science Foundation, and the U.S. Department of Energy Office of Science. The SDSS web site is http://www.sdss.org/.

Finally, thank you mom and dad for supporting me throughout my work on this thesis. I could not have done it without you.

Abstract

Astrophysical masers are natural microwave amplifiers by stimulated emission and when detected in galaxy centers, they are extremely luminous (i.e. millions of times more luminous than those associated with typical star-forming regions in the spiral arms of our own Milky Way). A fraction of water megamasers detected in 22 GHz emission in galactic nuclear regions are in a disk-like configuration, which makes them extremely valuable for providing direct geometrical distances to galaxies and the most precise and accurate masses of supermassive black holes. Nevertheless, these systems are extremely rare. While the exact mechanism of water maser emission production is not known, there is tentative evidence that the disk masing conditions are associated with accretion of matter onto black holes that are as massive as millions to billions of Suns, which is usually detected as active galactic nucleus activity. In particular, megamaser disk emission appears to be associated with the active galactic nuclei that are obscured by cosmic dust in their host galaxies' circum-nuclear regions. Improvements on their detection rates in future surveys rely on better understanding of their physical properties, in relation to those of their host galaxies. Using data from the *Wide-Field Infrared Survey Explorer* we systematically study the mid-infrared properties of the galaxies with and without nuclear water maser emission to better constrain the connection between water masing activity and the circumnuclear dust absorption and radiation reprocessing in galaxy centers.

1. Introduction – Water Megamasers and Galaxy Centers

1.1 Cosmic Maser Emission

Masers, which stand for *microwave amplification by stimulated emission of radiation*, occur naturally in the interstellar medium. They originate in high density gas (yet extremely low compared to terrestrial conditions; n(H_2) $\geq 10^7$ cm^{-3}) near a source of excitation, or generally, an energy source. Excited molecules and atoms decay radiatively, and produce a population inversion. As a consequence, the radiation is amplified, rather than absorbed, as it propagates through the medium. Moreover, the inverted medium occurs over a path length that is sufficiently long (AU to parsec scale) to produce significant amplification such that the intensities of the emission can be detected (Lo 2005).

At the fundamental level, the physics of astrophysical masers is similar to that of laboratory lasers. However, due to their strongly non-linear nature, the relation between the observed maser characteristics and the physical conditions of the masing medium, and thus the exact pumping mechanism, remain difficult to determine.

Astrophysical masers were first found in star forming regions and around evolved stars in the Milky Way Galaxy. Two of the most common types of masers found in our galaxy are cosmic OH and H_2O masers. These masers were found serendipitously because they had surprisingly large flux densities (Gundermann 1965; Weaver et al. 1965; Cheung et al. 1969). OH and H_2O masers are generally detected at peak frequencies of $\nu = 1.6$ GHz and 22.2 GHz, or wavelengths of $\lambda = 18$ cm and 1.35

cm, respectively. The OH and H_2O masers can have isotropic luminosities that can be as high as 1 solar luminosity ($L_\odot$) (Genzel & Downes 1977; Walker, Matsakis & Garcia-Barreto 1982). However, the mean luminosity for Galactic maser sources is only 10^{-4} $L_\odot$, with only a couple of masers known to have luminosities larger than 0.1 $L_\odot$ (Palagi et al. 1993).

Nevertheless, very powerful maser emission has been detected in the nuclear regions of some external galaxies (Dos Santos & Lepine 1979; Baan, Wood & Haschick 1982). These extragalactic masers can have luminosities ranging up to 450 $L_\odot$ (Claussen, Heiligman & Lo 1984; Claussen & Lo 1986). Given that the luminosities of some of these masers are on the order of 10^6 times greater than that of typical Galactic masers, these phenomena have been termed "megamasers."

1.2 Water Megamasers and Their Applications

Inspired by the parsec scale of a circumnuclear disk proposed to explain the polarized optical continuum and broad emission lines from active galactic nuclei (Antonucci & Miller 1985), and in analogy with the circumstellar disk proposed to explain masers around protostars (Elmegreen & Morris 1979), Claussen & Lo (1986) argued that the luminous water masers detected in galaxy centers could originate in dense gas clouds in a circumnuclear disk. The gas clouds would be excited by mass outflow from an active galactic nucleus (AGN), where the seed excitation is produced by the accretion disk of matter that swirls around a supermassive black hole (with masses between 10^6 and 10^9 solar masses ($M_\odot$); Salpeter 1964; Lynden-Bell 1969).

Evidence in favor of this model came from Very Long Baseline Interferometry (VLBI) and Very Long Baseline Array (VLBA) observations of NGC 4258, which revealed high-velocity features that were redshifted and blueshifted and spatially offset from the features of the systemic velocity (i.e., the relative velocity of galaxy NGC 4258 with respect to the Milky Way Galaxy). These velocity features reflect a nearly

planar structure. The velocity of the high-velocity features decreases with distance (r) from the center of rotation as $r^{-1/2}$ (Greenhill et al. 1995, Miyoshi et al. 1995, Moran et al. 1995). Basically, the VLBI and VLBA observations showed a nearly edge-on thin Keplerian disk, between the inner and outer radii of 0.13 pc and 0.26 pc, respectively (Figure 1, from Herrnstein et al. 1999).

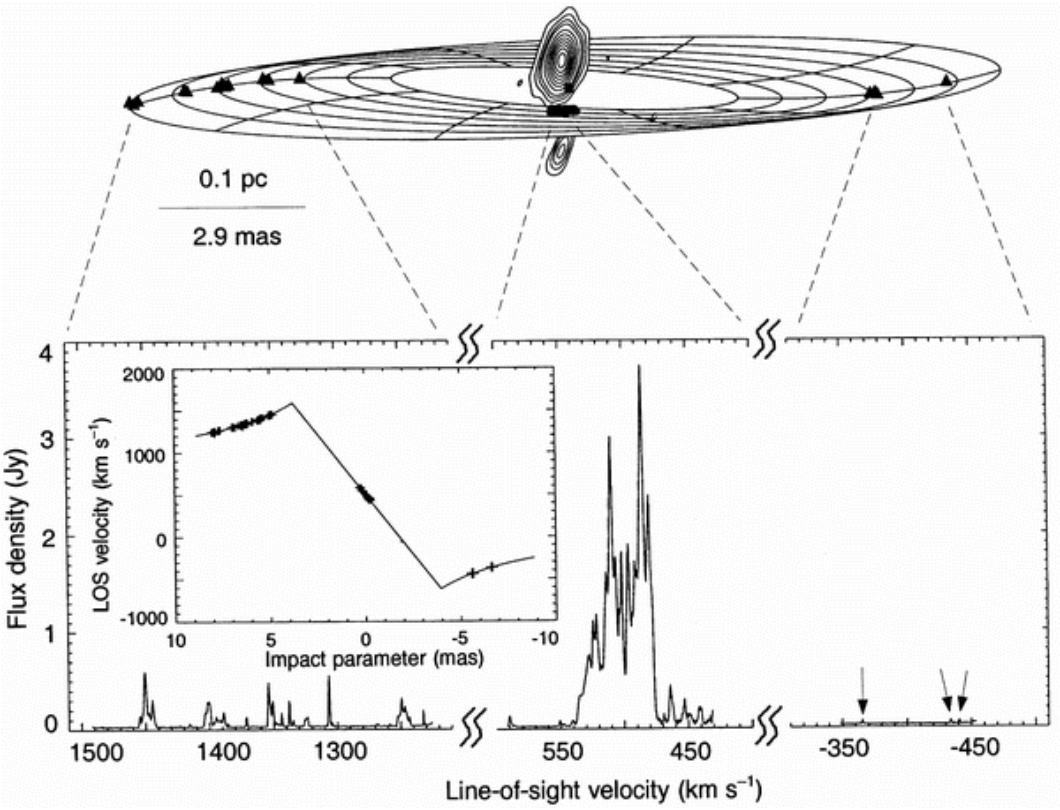

Figure 1.1: *Upper Panel:* A warped-disk model of the position of the water maser emission detected in NGC 4258, with North as the top. The contours represent VLBA continuum images. *Lower Panel:* The VLBA total power spectrum with the high-velocity features on either side of the systemic velocity (470 km s^{-1}). The inset shows the line-of-sight (LOS) velocity versus the impact parameter. The high-velocity masers trace a Keplerian curve to better than 1% (from Herrnstein et al. 1999).

The high-angular resolution of VLBI and the high temperature of water maser emission detected in NGC 4258 have made it possible to probe the nuclear regions of galaxies at unprecedented resolution, which is difficult to achieve by other means: at d = 7 Mpc, the angular resolution is ~ 300 μas. These observations have provided one

of the most compelling cases for the presence of supermassive black hole at the center of NGC 4258. Due to their well-measured Keplerian rotation, water megamaser disks are the closest to an optimal dynamical tracer of the central mass lurking in galaxy centers.

Megamaser disks prove immensely valuable not only because they can probe the inner workings of the AGN systems or for providing the most accurate masses of supermassive black holes. The maser disks also offer the most promising prospect for obtaining a highly accurate value of the Hubble Constant H_0 at $z = 0$ via direct geometric angular diameter distance measurements, in a single step. This method provides essential alternatives to indirect methods that use standard candles and distance ladders (e.g., Reid et al. 2012). Therefore, by using the water megamaser disks to calculate distances, astronomers can constrain the cosmological models. This will help determine the Hubble constant H_0 to within a 3% accuracy, which would provide the arguably best single constraint on the nature of Dark Energy (DE) where its effect is greatest (Hu 2005; Olling 2007).

Extending measurements similar to those performed for the water maser system in the center of NGC 4258 to more galaxies and to larger distances is very important. Therefore, there is strong motivation to search for additional luminous circumnuclear H_2O masers.

1.3 Surveys of H_2O Megamasers

In the last several decades, water masers were discovered serendipitously in various galaxies. Current water maser surveys are run by the Megamaser Cosmology Project (MCP; Reid et al. 2013; Kuo et al. 2013, 2015). The MCP is an international collaboration that aims to determine the Hubble constant H_0 by measuring the geometric distances to galaxies using water megamaser disks as dynamical tracers around the central black hole. The MCP makes publicly available the largest sample of galaxies

surveyed in 22 GHz water maser emission. Out of over 3500 galaxy nuclei surveyed to date, only about 160 nearby galaxies are found to host water masers (based on up to date results of all 22 GHz surveys of galaxies via the MCP)[1]. Of the galaxies with water maser emission, $\sim 70\%$ host water megamasers disks and only about 40% of these megamaser systems have distinct "triple" spectra displaying systemic and high-velocity emission in three line complexes, suggestive of a disk-like configuration (Gao et al. 2016). Only about five of these megamaser disks lie at distances $D > 50$ Mpc, which are needed to calculate distances that will help constrain the Hubble constant (Braatz, Wilson & Henkel 1996, 1997; Braatz et al. 2004; Kuo et al. 2011).

In addition, the current megamaser surveys do not appear to improve the number statistics of such sources. In order to make current searches more efficient and effective, it is necessary to have a good understanding of the physical characteristics that provide the right environments for water maser emission in galaxy centers. However, this information remains ambiguous. There is some evidence that water megamaser disk activity may be associated with the molecular disk that surrounds the actively accreting central supermassive black hole harbored by an AGN. This is because dust in this torus is thought to provide similar conditions to those that are necessary for water maser emission such as the presence of a high density environment that is heated by a nearby source of energy (Braatz, Wilson & Henkel 1996a, 1997; Braatz et al. 2004). However, some megamasers are also detected along jets protruding long distances from the nucleus, and the origin of other megamasers remains ambiguous.

Thus, it is not clear that water megamasers are always produced in association with an AGN, or whether the maser emission is associated with unrecognized AGN (i.e., low-luminosity or obscured AGN). It is also possible that the megamaser activity is connected to other nuclear properties of the host galaxies. However, in order

[1]http://wiki.gb.nrao.edu/bin/view/Main/MegamaserCosmologyProject

to better understand the physical nature of maser emission in galaxy centers, we need improved statistics on the presence of megamaser disks in galaxy nuclei. This understanding could help answer questions such as: Are megamaser disks always related to black hole accretion? Is maser activity related to the mass of the black hole, the accretion rate, X-ray sources, or other small-scale properties of the galaxy nucleus? Do they require the presence of a dusty or molecular torus? What is the true detection rate of megamaser disk emission?

1.4 This Thesis: Connecting Mid-IR Emission with Water Maser Activity

This project aims at improving the current understanding of properties of galaxies that host water megamaser emission, which should make the search for the elusive megamaser disks more efficient. The all-sky survey carried out by the *Wide-field Infrared Survey Explorer* (*WISE*; Wright et al. 2010) has opened up a new window in the search for obscured AGNs, which are believed to provide the necessary conditions for water megamaser emission. The optically hidden AGNs are expected to exhibit characteristically red mid-infrared colors originating in the reprocessed radiation by the surrounding obscuring dust. Thanks to exposures at W1=3.4 μm, W2 = 4.6 μm, W3 = 12 μm, and W4 = 22 μm, WISE can provide color diagrams like W1–W2 vs. W2–W3, which are found useful to separate obscured AGNs from normal star-forming galaxies with bluer colors in the nearby universe (Figure 1.2). Comparisons with previous investigations of AGN properties in IR provide useful WISE color cuts, which can be associated with spectral energy distributions characteristic of dusty red accreting galaxies, and thus a novel way of detecting these systems (e.g., Stern et al. 2012; Assef et al. 2013).

Given that the redshifts of the galaxies in the current samples of galaxies surveyed for water maser emission are low, and that for $z \approx 0$, *WISE* color selections are

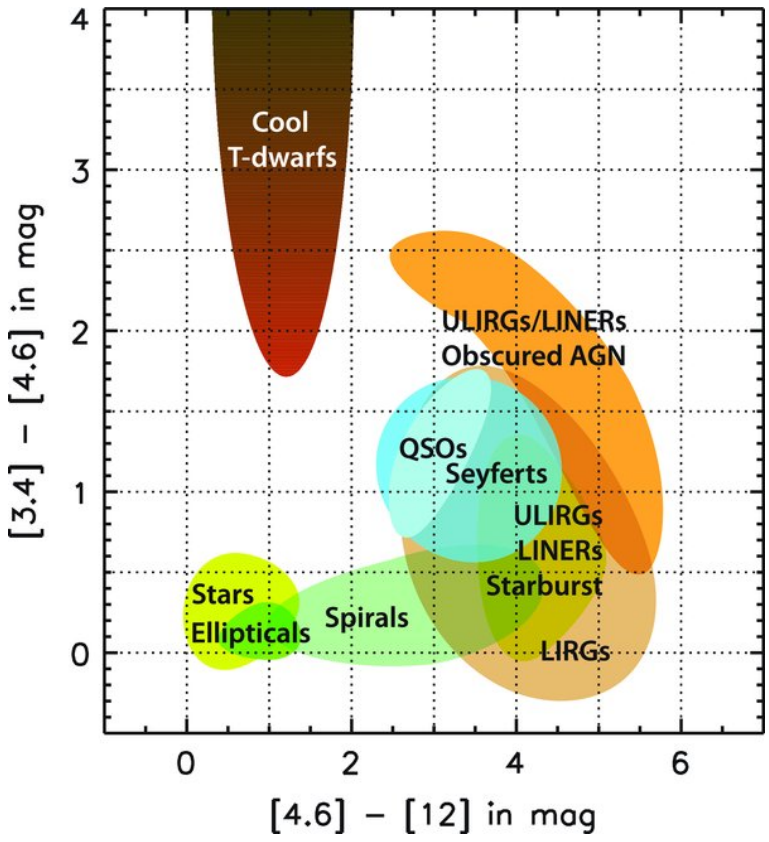

Figure 1.2: *WISE* W1–W2 versus W2–W3 color-color diagram showing the locations of various types of objects in this parameter space. Water megamaser disks are thought to be associated with red Seyferts and obscured AGN (from Wright et al. 2010).

critically sensitive to the AGN's power relative to that of the host galaxy, this project explores the water maser detection in relation to the range of *WISE* properties and the proposed color cuts for AGN emission. This study should provide the essentials for refinement of future water megamaser surveys and also for constraining the dominant ionization mechanism most likely associated with water maser activity.

Throughout this paper, we adopt an $\Omega_M = 0.3$, $\Omega_\Lambda = 0.7$, and $H_0 = 70$ km s^{-1} Mpc^{-1} cosmology.

2. The Data: Detection of Masers, Megamasers, and Disks and their *WISE* Counterparts

2.1 Galaxies Surveyed in 22 GHz for Maser Emission

The largest and most comprehensive catalog of all galaxies surveyed for water maser emission in 22 GHz is being compiled and made publicly available by the Megamaser Cosmology Project (MCP; Reid et al. 2009; Braatz et al. 2010). The catalog has been updated on a regular basis to include all of the new observations and associated findings. For this thesis, we limit our study to the MCP data compiled by May 2013, which includes a total of 3490 galaxies surveyed for maser emission in 22 GHz, out of which 151 ($\sim 3\%$) are found to host maser activity. Of the detected masers, $\sim 70\%$ have water luminosities that are at least ten times the Sun's luminosity, and are therefore megamasers. Masers with water luminosities that are not powerful enough to be considered megamasers are called kilomasers. Approximately 40% of the megamasers exhibit both the systemic and the high-velocity redshifted and blueshifted features, suggesting that they originate in disk-like configurations (Figure 1.1). This amounts to very few galaxies with water megamaser disks ($\sim$30 total).

In the MCP catalogs, the data for all the galaxies surveyed for H_2O maser emission are presented in the form of an atlas comprising sky positions, recession velocities, 22 GHz spectra, the sensitivity of each observation, and the corresponding source brightness temperature. Herein, we refer to galaxies with confirmed H_2O maser emission as maser galaxies or masers, and to galaxies with no maser detection as non-maser

galaxies, or non-masers. For the maser galaxies, the MCP catalogs also include the maser luminosities, morphologies, and the corresponding discovery reference.

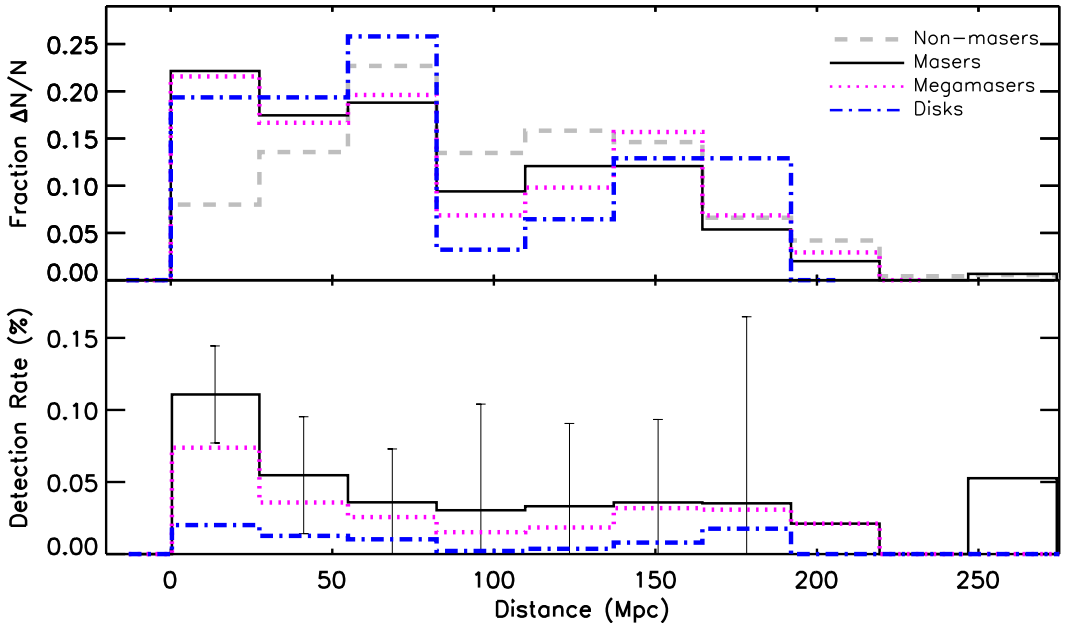

Figure 2.1: *Top panel:* Normalized number of masers and non-masers in the MCP sample as functions of distance. *Bottom panel:* Detection rates of the samples as a function of distance.

Figure 2.1 presents a summary of the number statistics of the samples of maser and non-maser galaxies as a function of distance. The upper panel shows the normalized distributions of non-masers (dashed gray), masers (continuous black), and the subgroups of megamasers (dotted magenta) and disks (dot-dashed blue). ΔN is the number of objects in a given sample in a distance bin while N is the size of the sample. The lower panel shows the detection rates of masers, megamasers, and disks, out of all the galaxies surveyed for water maser emission. Uncertainties in the detection rates are only shown for the whole maser sample, and only for bins with more than three objects. As it is readily apparent from these distributions, the majority of the maser galaxies have been detected within 150 Mpc, and the detection rate decreases with increasing distance. Nevertheless, at distances larger than 50 Mpc, the statistics are

not high enough to determine with confidence or quantify the distance dependence.

2.2 A few notes on the Maser Selection Effects

It is important to note that, to date, the surveys for maser activity in extragalactic sources focused mainly on narrow-lined (type 2) AGNs, Seyfert galaxies or Low Ionization Nuclear Emission Regions (LINERS). The reason behind this choice comes from the early detections of luminous megamasers that were found exclusively in well known type 2 AGN, where the maser emission originates within about 1pc (3 light-years) or less of the nucleus (e.g., Claussen & Lo 1986; Haschick et al. 1994), and the idea that masers might trace molecular material associated with a dusty torus that surrounds the nucleus and thus obscures the central engine (BH, accretion disk, and the broad line emission region) for large inclination angles (the "Unification scenario;" Antonucci & Miller 1985). While this scenario appeared to be confirmed by VLBI observations of the megamaser in NGC 4258 (Miyoshi et al. 1995; Greenhill et al. 1995; Lo 2005), there are still open questions about how exactly the obscuring torus and the masing disk are related. For example, the H_2O megamaser emitting quasar MG J0414+0534 shows broad emission (Impellizzeri et al. 2008), proving that broad-lined (type 1) AGNs could also host megamaser disks, meaning that either the presence of a torus does not play as crucial a role as originally thought, or that the AGN unification scenario needs refinement.

Also, for a large number of galaxies, determining the AGN nature of their nucleus is not trivial. Optical emission-line ratio diagnostics (e.g., Baldwin, Phillips & Terlevich 1981, Veilleux & Osterbrock 1987, Kewley et al. 2006; Figure 2) that have been quite successful in identifying cases where the dominant ionization mechanism is either accretion onto a black hole (i.e., Seyferts) or radiation from hot, young stars (i.e., H II nuclei), remain inconclusive for the majority of LINERs and objects that straddle the borders between starburst galaxies and AGNs. This leaves the faint end

of the AGN luminosity function unconstrained, meaning that the true incidence of massive BHs in the present universe remains unknown, and it is not clear to what degree the ambiguity is due to the strength of the AGN, the surrounding dust obscuration, or contamination by the host stellar light. Therefore, restricting the maser searches to optically identified type 2 AGNs could have caused the surveys to overlook a potentially significant portion of the water megamaser disks.

Recognizing these trends is important when compiling and analyzing maser detection rates, and for trying to identify what galaxy types or characteristics associate most strongly or intimately with the maser emission. Systematic studies of the properties of the maser galaxies, and comparisons with their non-maser analogs have been conducted at optical wavelengths (Zhu et al. 2011; Constantin 2012, van den Bosch et al. 2016), in 2-10 keV (Greenhill et al. 2008, Zhang et al. 2006, Zhang et al. 2010), and radio continuum (Zhang et al. 2012, Liu et al. 2017). The results of these studies reveal differences between masers and non-masers, albeit with great scatter, and make great strides towards designing more efficient targeting of maser galaxies. Nevertheless, given the biases described above, the degree to which some of these results identify with a strong connection between the masing and Seyfert activity remains unclear. A mid-infrared characterization of the galactic maser emission should offer new insights, especially in light of the measurements provided by *WISE*.

2.3 *WISE* Matches for MCP Samples

WISE mapped the sky at 3.4, 4.6, 12, and 22 μm (W1, W2, W3, W4) in 2010 with an angular resolution of 6.1", 6.4", 6.5", and 12.0" in the four bands, respectively. *WISE* achieved 5σ point source sensitivities better than 0.08, 0.11, 1 and 6 mJy in unconfused regions on the ecliptic in these four bands, respectively. Sensitivity improves toward the ecliptic poles due to denser coverage and lower zodiacal background.

The *WISE* Source Catalog contains information for 563,921,584 point-like and resolved objects detected on the Atlas Intensity images. Catalog sources are required to have a measured signal-to-noise ratio of SNR > 5 in at least one band. The source catalog includes: J2000 positions, photometry, uncertainties, measurement quality flags and extended source and variability flags in the four *WISE* bands, along with associated information cross-referencing *WISE* sources with the 2MASS Point and Extended Source Catalogs.

We matched the MCP samples of maser and non-maser galaxies to the public all-sky *WISE* source catalog at NASA/IPAC Infrared Science Archive[1] via the IRSA[2] catalog tool. We ask in our queries for all *WISE* detections whose positions agree to the MCP positions within 3 arcseconds, and we require that the *WISE* matches to MCP galaxies are detected at better than 3σ in both the 3.4μm and 4.6μm bands (W1 and W2 respectively), which are used to identify and classify these galaxies as AGN based on the W1–W2 color (see Figure 1.2). We also require for the matches to have signal-to-noise ratios of SNR ≥ 3 in the W4 band. We did not restrict the detection SNR in the W3 band because galaxies that meet our requirements in W4, which is the least sensitive band, will generally have higher signal-to-noise detections in the W3 band. For the cases where the queries produced multiple *WISE* matches within a 3 arcsecond search radius around individual MCP sources, we kept only the *WISE* match with the closest separation. For all duplicates, we visually inspected the closest *WISE* match in all four *WISE* bands to make sure that it corresponds to the MCP source.

The results of the cross-matching between the MCP and *WISE* Source catalogs are summarized in Table 2.1. We list here the total number of masers, megamasers, and disks from the MCP catalogs along with their associated *WISE* matches. All of

[1]http://wise2.ipac.caltech.edu/docs/release/allsky/
[2]http://irsa.ipac.caltech.edu/Missions/wise.html

Table 2.1: Cross-matching results between the MCP and *WISE* catalogs

Sample	All Masers	Megamasers	Disks	Non-Masers
MCP	151	102	32	3339
MCP-*WISE*	134	102	32	2767

the megamasers and disks are found to have a *WISE* counterpart while the kilomasers only have a 90% *WISE* match; only 85% of the non-masers are detected in *WISE*. We expect the megamasers and disks to have mid-IR counterparts because they most likely originate in the dusty torus, which emits in the mid-IR regime. However, due to selection bias, most of the maser disks have been detected in Seyfert galaxies, and it is unclear whether these Seyferts differ from other Seyferts in their mid-IR emissions due to properties related to the maser emission.

3. The *WISE* Properties of Maser and Non-Maser Galaxies

One step towards improving the megamaser disk detection rates is to determine the mid-infrared properties that distinguish between masers and non-masers. The most basic data we have available are the magnitudes of the MCP-*WISE* samples in the four *WISE* bands, and we provide here a first look at how these magnitudes compare for the different samples of masers and non-masers. Figure 3.1 shows W1 vs. W2, W1 vs. W3, and W1 vs. W4 magnitude-magnitude diagrams along with calculations of maser detection rates in each *WISE* band. In all scatterplots, there is a significant overlap in the masers and non-masers, however, the W1 vs. W3 and W1 vs. W4 diagrams reveal a more pronounced separation between these samples. The locus of masers, megamasers, and disks appears shifted towards brighter magnitudes (lower values) in W3, W4, and possibly in W1 as well. There is no obvious difference between the magnitudes of masers and non-masers in W2.

Guided by these apparent separations, by the detection rates in bins of magnitudes shown in the histograms, and with the goal of separating out as many megamaser disks as possible, we constructed a set of magnitude cuts that delineate the regions with lower numbers of non-masers and thus with increased maser detection rates. These cuts are shown by vertical and horizontal lines in each panel and are summarized in Table 3.1. Folding these magnitude cuts into possible survey criteria for water masers, we find that the maser detection rate can be increased by $\approx 50\%$ (an increase from 3% to 5-6% for all masers, from 3% to 4-5% for all megamasers, and from 0.9% to 1.5% for all disks). Applying all these cuts simultaneously produces similar increases

in the maser detection rates. The greatest improvement in the maser detection rate is found with the combination of the W1<12.7 and W4<7.1, suggesting that future maser surveys can clearly benefit from these criteria.

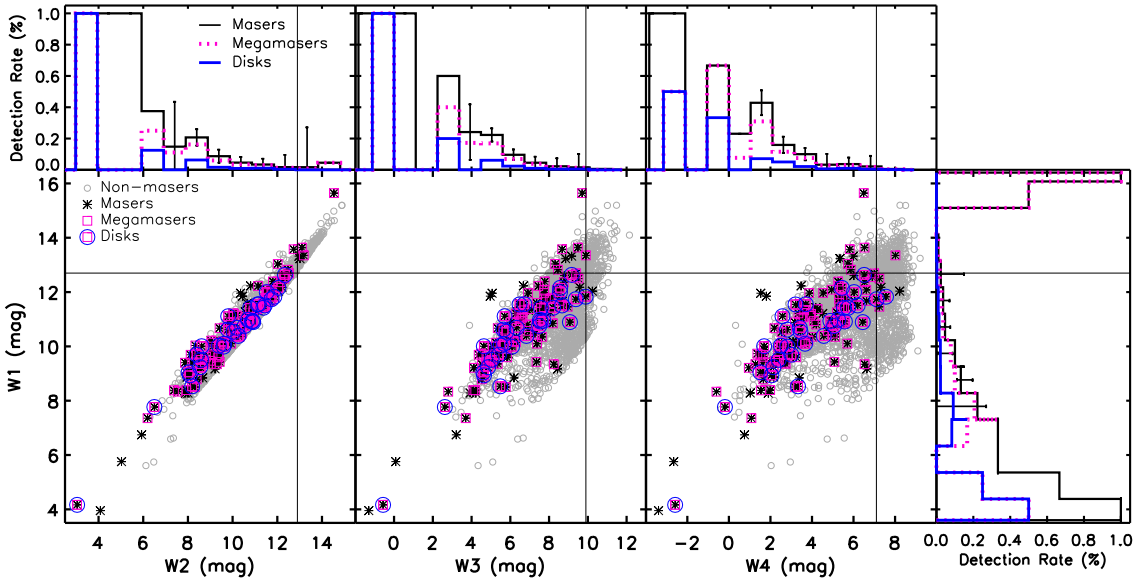

Figure 3.1: Magnitude-magnitude diagram for the MCP-*WISE* samples of masers (black asterisk), megamasers (magenta square), disks (blue circle), and non-masers (gray circle). Magnitude cuts in all four bands are shown as black lines in both the magnitude plots and histograms. Histograms for each magnitude show the detection rates for each sample in each magnitude bin.

Table 3.1: Maser detection rates for various combinations of *WISE* magnitude cuts. The detection rates were calculated out of 3490 galaxies surveyed in 22 GHz.

MCP Samples	$W1 \leq 12.7$ $W2 \leq 12.9$	$W1 \leq 12.7$ $W3 \leq 9.9$	$W1 \leq 12.7$ $W4 \leq 7.1$	All Cuts Simultaneously
All Masers	5.1%	5.2%	6.1%	6.1%
Megamasers	3.9%	4.0%	4.7%	4.7%
Disks	1.3%	1.3%	1.5%	1.5%

Given that mid-IR colors prove to be useful in distinguishing between various types of galaxies (Fig. 1.2), we also look at how our samples compare in various magnitude-color diagrams. We show in Figure 3.2 three magnitude-color diagrams along with

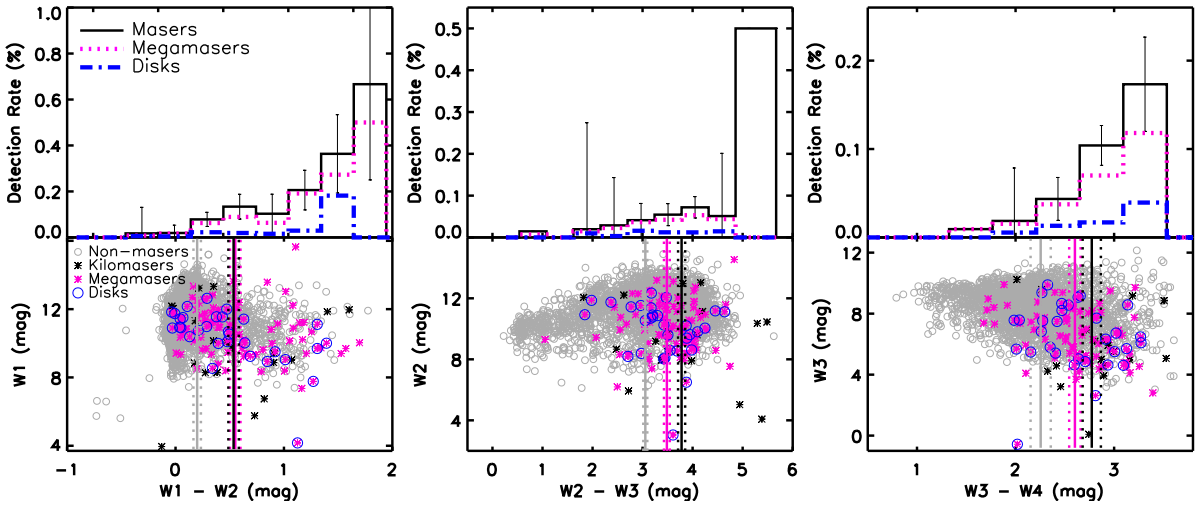

Figure 3.2: MCP-WISE magnitude-magnitude diagrams and maser detection rates as functions of color. The upper panels show the detection rates with uncertainties in the maser detection rates. The lower panels show the distribution of the samples' magnitudes as functions of the *WISE* colors. The solid lines show the average color for the non-masers, kilomasers, and megamasers and the dotted lines represent the standard deviation for each average color.

the detection rates in the W1–W2, W2–W3, and W3–W4 colors[1]. For each of these magnitude-color diagrams, we indicate (with vertical lines) the average colors for the non-masers, kilomasers, and megamasers. We find that in average the non-masers are significantly bluer (lower values of colors) than the masers. Interestingly, within the maser galaxies, at least in the longer wavelength colors (W2–W3 and W3–W4), it is the kilomasers that are the reddest.

Table 3.2 lists the average colors with their associated standard deviations. The average W1–W2 values show no significant difference among the different types of masers. On the other hand, for the other two colors, the megamasers and the disks distinguish themselves from the kilomasers, by exhibiting bluer colors. W2–W3 shows the most significant differences between the different types of masers, with the disks appearing to be the bluest of the megamasers; the non-masers remain distinctly bluer

[1]A color represents the difference between two magnitudes.

Table 3.2: Mean and standard deviations of the *WISE* colors presented in Figure 3.2. The maser, kilomaser, megamaser, and disk detection rates for each of the average colors within the standard deviation boundaries are given in parentheses. The megamasers have been bolded to highlight the significantly high detection rates.

MCP-*WISE* Samples	W1–W2	W2–W3	W3–W4
All Masers	0.55±0.05 (11%)	3.53±0.06 (5%)	2.65±0.06 (7%)
Kilomasers	0.54±0.05 (3%)	3.81±0.07 (2%)	2.80±0.09 (4%)
Megamasers	**0.55±0.05 (8%)**	**3.49±0.06 (5%)**	**2.60±0.06 (16%)**
Disks	0.51±0.07 (3%)	3.39±0.09 (2%)	2.60±0.07 (2%)
Non-masers	0.20±0.03	3.05±0.04	2.25±0.10

though. Thus, while red *WISE* colors appear to be a way of searching for water maser emission in galaxies, the megamaser disks do not distinguish themselves by extreme redness. Targeting the reddest galaxies appear efficient for finding maser galaxies, however, this will only recover a fraction of the megamaser disks.

Nevertheless, if a narrow color interval centered on the average values is considered, then the detection rate of megamasers increases significantly. We have calculated the detection rates for the color intervals centered on the average values and with widths matching the standard deviation; we list these numbers in parentheses in Table 3.2. The detection rates for the megamasers are indicated in bold to emphasize the great differences this particular selection may produce. When only these narrow color intervals are considered, the detection rates for the megamasers in particular increase dramatically from an overall detection rate of <3% to 8% in W1–W2, to 5% in W2–W3, and to 16% in W3–W4. The disk detection rates also double.

Because the megamaser disk detection rates increase dramatically for these narrow color intervals, we could use them as another way to search for more disks. The challenge comes from identifying all galaxies with *WISE* colors within the desired average color intervals. While previous maser surveys have exhausted the samples of spectroscopically identified galaxies, there is a significantly higher number of galaxies

with photometric redshifts that have not yet been surveyed for water maser emission. A new sample of megamaser disk candidates can be built by searching the SDSS database for all galaxies with photometric redshifts, and then by cross-matching with the *WISE* catalogs to select the ones whose mid-IR colors correspond to the largest maser detection rates, as predicted by the above calculations.

We performed this search and found 912,821 objects classified by SDSS as galaxies with photometric redshift values < 0.3 to reflect the redshift range of the MCP samples, which matches the current sensitivity limits of the available radio detectors, and for which the fractional error in photometric redshift is less than 50%. The *WISE*-IPAC database reveals 64 galaxies with *WISE* colors that fall within the desired megamaser average color intervals. With a predicted detection rate of 8% in W1–W2, 5% in W2–W3, and 16% in W3–W4, we expect to find ~ 5 megamasers; similarly, based on predicted detection rates of 3% in W1–W2 and 2% in W2–W3 and W3–W4, it is possible that $\sim$2 more disks are hidden among galaxies of these particular colors.

4. The Maser-AGN Connection as seen by *WISE*

A possible connection between the megamaser disk activity and accretion onto supermassive black holes at the center of the maser disk has been put forward ever since the discovery of the first megamaser disk (NGC 4258; Herrnstein et al. 1999). One of the main conditions required for maser amplification, i.e., high column density along the line of sight, explains the association with narrow line (type 2) AGN (e.g., Braatz et al. 1997b; Kondratko et al. 2006), and in particular Compton-thick systems (e.g., Greenhill et al. 2008; Zhang et al. 2010; Castangia et al. 2013). The other important ingredient for maser emission, the heating that drives a population inversion, is not necessarily solely provided by accretion in an AGN. Shocks and strong star formation activity can also achieve the same result (e.g., Lo 2005). Thus, it is still a matter of debate whether the AGN and maser disk activity go hand in hand, as well as whether the origin and survival of maser disks are dependent on actively accreting SMBHs.

Assuming that all megamaser disks are associated with SMBH accretion, we would need to understand why some types of AGNs are more prone to hosting maser disks than others, even within those classified as type 2. It is by no means clear how the obscuring torus and the masing disk are related. The masing disk could be the innermost part of a molecular accretion disk adjacent to the torus, or it could just be the thin, central plane of the torus in which the column density is high enough for strong amplification. Alternatively, it might also be dynamically independent from the torus, with a strong misalignment between their axes. The fact that, e.g., the H_2O megamaser emitting quasar MG J0414+0534 shows broad emission (Impellizzeri

et al. 2008) proves that broad-lined AGNs could also host megamaser disks, meaning that either the presence of a torus does not play as crucial a role as originally thought, or that the AGN unification scenario needs refinement.

Moreover, for a large fraction of nearby galaxies, finding the dominant ionization power of their nuclei, and thus accurately identifying an AGN remains challenging: their optical spectra reveal line flux ratios that straddle the borders between starburst galaxies and AGNs (e.g., Filippenko & Sargent 1985; Constantin et al. 2015), their X-ray emission remains just short of the secure AGN limit of 10^{42} erg/s (e.g., Constantin et al. 2010; Netzer 2015), and their radio morphologies remain consistent with compact emitters for only a small fraction (Merloni 2015). Also, while maser detection is highest among Seyferts ($\sim$8%; Braatz et al. 2004), it has been shown that this might not be due entirely to a genuine connection to this type of activity, as it may be enhanced by the biases associated with the recent maser surveys that targeted almost exclusively type 2 Seyferts, and that the maser detection rate is non-zero for non-AGN types (Constantin 2012). Thus, we do not know yet whether megamaser disks are always related to black hole accretion, or whether they require a dusty/molecular torus. If this torus is necessary for strong maser disk emission, would the properties of the dusty torus be similar or different among all megamaser disks? Would they reflect similar or different temperature ranges, and thus different mid-IR spectral energy distributions (SEDs) and colors? Would any similarities or differences in their mid-IR SEDs help us build more efficient maser disk surveys? We explore these connections in the following subsections.

4.1 Mid-Infrared SEDs for Masers and Non-Masers

Different physical processes that might power the galaxy centers leave potentially different imprints on the global and detailed shape of their observed SEDs, each dominating at different wavelengths. The four mid-IR bands provided by *WISE* have

been shown to be somewhat useful in distinguishing between some of the potential dominant power sources (e.g., Assef et al. 2010): there is a major difference in the SEDs of AGNs and normal galaxies in that the former have a minimum at 1-2 μm (systems with strong nuclear heating tend to be roughly a rising power law in their mid-infrared SEDs), while non-active galaxies have a peak (i.e., the opacity peak of the stellar emission at 1.6 μm). Moreover, star-forming and passive galaxies can be distinguished from their longer wavelength data ($>\approx 4\mu$m), where the intense star formation episodes are associated with a significant amount of dust reprocessing, which will make these systems luminous (or ultra luminous) IR galaxies (e.g., ULIRGs, Sanders & Mirabel 1996).

We explore here the connection between the presence and morphology of the water maser emission and the mid-IR SED shape of their hosts. We constructed the SEDs for all the masers and non-masers and we show them in Figure 4.1. The

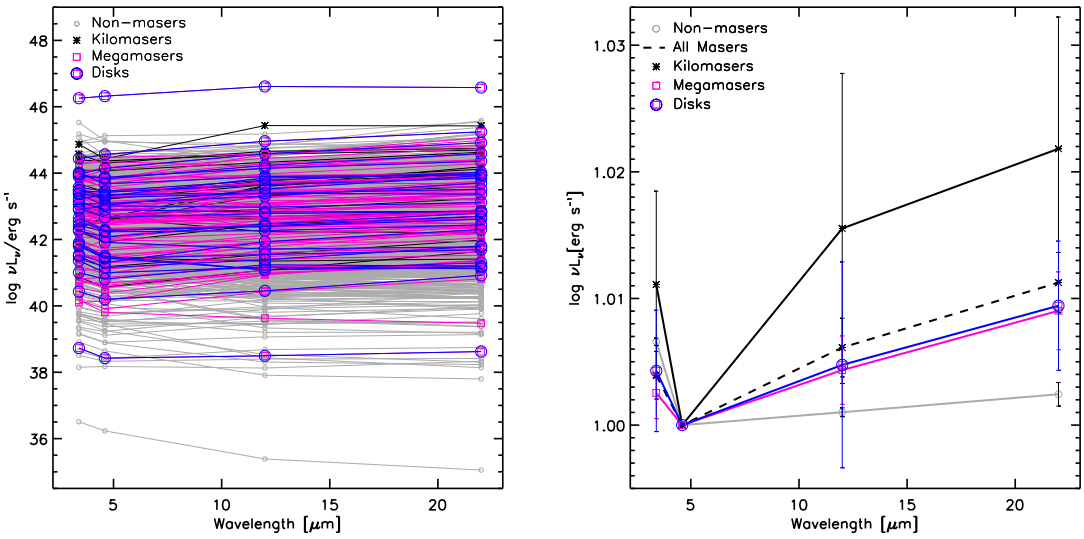

Figure 4.1: *Left*: νL_ν versus wavelength for the MCP-*WISE* kilomasers (black), megamasers (magenta), disks (blue), and non-masers (gray). *Right*: Average luminosities normalized to the average maser W2 luminosity for SEDs with the same groups from the left panel, to which we added for comparison the normalized SED for the sample of all maser galaxies (black dashed line).

WISE fluxes for each galaxy were calculated using the magnitude to flux conversion method described in Wright et al. (2010), and the luminosities were calculated using the distances derived from their systemic velocities as listed in the MCP catalogs.

The left panel of Figure 4.1 shows all of the individual SEDs for the kilomasers (black asterisk), megamasers (magenta square), disks (magenta square with blue circle, blue line), and non-masers (gray circle). The total mid-IR luminosities L_{WISE} are given by the area under each curve; the averages per sample are presented in Table 4.1. The shape and strength of the SEDs for masers and non-masers show significant overlap, however, there are some apparent differences. In terms of the spread of the SEDs and thus their L_{WISE}, the masers occupy a more compact range than the non-masers; the kilomasers exhibit the narrowest luminosity range (10^{40} to 10^{45} erg/s). Also, it is pretty clear that the maser galaxies are more luminous in mid-IR than

Table 4.1: Average mid-IR integrated luminosities $< L_{WISE} >$ along with their associated standard deviations of the mean for the samples of kilomasers, megamasers, disks, and non-masers.

Sample	$< L_{WISE} > /(10^{44}$ erg s$^{-1})$
All Masers	1.7 ± 0.4
Kilomasers	5.1 ± 2.3
Megamasers	1.3 ± 0.3
Disks	1.4 ± 0.3
Non-masers	0.5 ± 0.09

the non-masers ($< L_{WISE} >_{\rm masers} = 1.7 \pm 0.4$ vs. $< L_{WISE} >_{\rm non-masers} = 0.5 \pm 0.09$). Interestingly, it is the kilomasers that have the highest average luminosity. The megamasers and their subgroup of disks remain similar in their mid-IR total power output, which is in between that of the kilomasers and the non-masers. Nevertheless, there are a few significant outliers: the object with the highest luminosity in each of the four *WISE* bands is a disk maser galaxy (NGC1068) rather than a kilomaser, and the least mid-IR luminous maser is also a disk (J0437+6637). Thus, while targeting

more mid-IR luminous galaxies is bound to return a higher fraction of maser-emitting systems (see Table 4.2), the disk masers do not show any useful peculiarity in their L_{WISE}.

Table 4.2: Fractions of all maser types within luminosity ranges; detection rates are indicated in parentheses.

Luminosity Range	All Masers	Kilomasers	Megamasers	Disks
$L_{WISE}/(\text{erg s}^{-1}) < 10^{41}$	9.0% (18%)	2.0% (1.5%)	9.8% (15%)	6.3% (3.1%)
$10^{41} < L_{WISE}/(\text{erg s}^{-1}) < 10^{44}$	82% (4.0%)	29% (0.5%)	83% (3.1%)	81% (1.0%)
$10^{44} < L_{WISE}/(\text{erg s}^{-1}) < 10^{46}$	8.2% (10%)	8.2% (3.7%)	5.9% (5.6%)	6.3% (1.9%)

To better emphasize the differences in the SED shapes, we show in the right panel of Figure 4.1 the average SEDs for each of the subtypes of masers and for the non-masers, by normalizing to the average maser luminosity in the W2 band; the samples are presented with the same symbol colors as in the left panel, and we also show for comparison the average SED for the sample of all masers with a black dashed line. This comparison reveals that non-masers have a relatively flat SED in the longer mid-IR wavelengths while all of the maser types exhibit clear rises in luminosities. The kilomaser subsample shows the most dramatic change in νL_ν for both longer and shorter wavelengths relative to the W2 band: in average, the kilomasers have the reddest W2–W3 colors, but also the bluest W1–W2 colors. Blue W1–W2 colors are usually associated with star-forming regions, which are expected to be prominent in kilomaser galaxies (Lo 2005; Ott et al. 2013); thus, the red W2–W3 colors for these objects would not necessarily be linked to dusty/obscured AGN activity, but simply to hot dust surrounding stellar nurseries.

On the other hand, the megamasers and their subgroup of disks show very similar average SED shapes: in contrast with the kilomasers, they are exhibiting the reddest W1–W2 colors while showing clearly redder W2–W3 colors than the average non-masers. These average trends support the previously proposed association

of megamaser emission with AGN activity as their dominant excitation is consistent with a rising power law towards longer wavelengths; nevertheless, contamination by star-formation cannot be ruled out, especially since the differences in the average SED shapes are not statistically significant (the error bars overlap).

4.2 Masing Activity & AGN classification based on *WISE* Color Selection Criteria

Previous studies found that we can detect a large portion of the population of red/dusty AGNs that do not show AGN-like optical signatures by using the *WISE* W1–W2 vs. W2–W3 color diagrams. We explore here through these methods the connection between obscured AGN activity and the H_2O masing phenomenon.

Mid-IR color cuts proposed for selecting red AGNs include W1–W2 ≥ 0.5 (Ashby et al. 2009), W1–W2 ≥ 0.8, for a lower contamination by non-active galaxies (Stern et al. 2012), and a set of criteria involving both of these *WISE* colors, with an even more stringent control for non-AGN contamination by Jarrett et al. (2011). Figure 4.2 illustrates the location of all of our MCP objects in the (W1–W2, W2–W3) color-color space, along with these AGN cuts.

If there is a strong association between megamaser and disk emission and obscured AGN activity, then we expect to see most of these systems with *WISE* colors of W1–W2 ≥ 0.8 or within the Jarrett et al. (2011) box, with most of the non-masers falling below the W1–W2 = 0.5. It seems however that this is not immediately the case: the masers and non-masers occupy color-color regions that overlap considerably. The distributions of both maser and non-maser galaxies follow the expected spread of galaxies (Wright et al. 2010), and there is no clear delineation of *WISE* galaxy colors that can be associated with the masers. The only possible difference is in their average W2–W3 color, which is clearly redder for the masers (<W2–W3> is 3.53 ± 0.06 for masers and 3.05 ± 0.04 for non-masers; see Table 3.2).

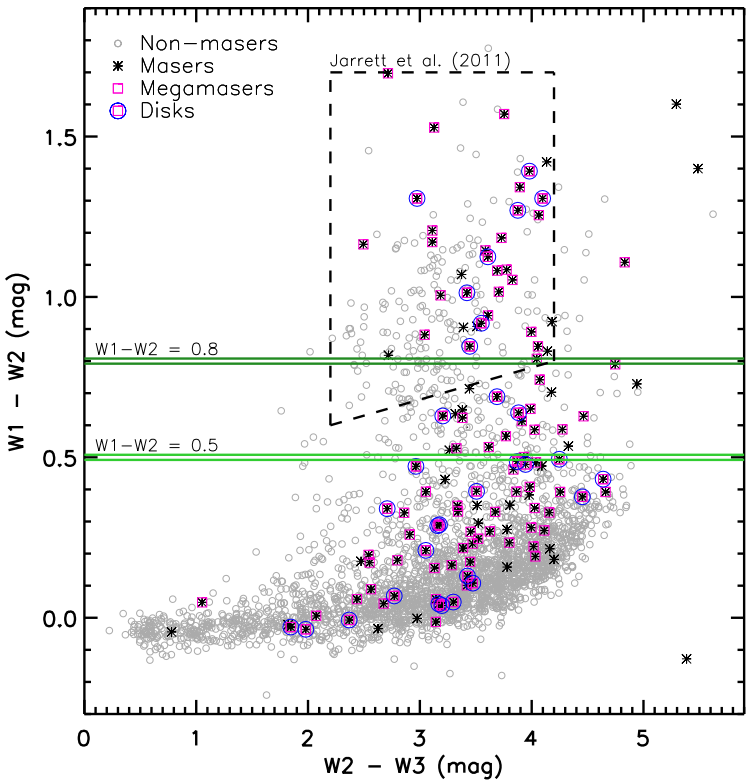

Figure 4.2: Color-color diagram of the MCP-*WISE* samples of masers and non-masers with color cuts for *WISE*-AGN selection: W1–W2 $\geq$ 0.5 (light green), Jarrett et al. (2011) (dashed), and W1–W2 $\geq$ 0.8 (dark green). Symbols are as defined in Figure 3.1.

We present in Table 4.3 the fractions of each maser subsample within the *WISE* AGN cuts discussed above, along with the corresponding detection rates. It is pretty clear that only $<\sim$1/3 of maser galaxies, and in particular megamasers and disks, fall into the red *WISE* AGN category, regardless of which criteria are used. Thus, the majority of the disk megamasers do not seem to be associated with obscured AGN activity. More than 50% of the megamaser galaxies exhibit blue *WISE* W1–W2 colors. On the other hand, the maser detection rates skyrocket in the red AGN regime. The overall maser emission appears to be 20% detectable among these sources, with a very high proportion of them being megamasers and disks. Thus, if galaxies with W1–W2$>$ 0.8 are targeted for maser emission, their detection rate is expected to reach

Table 4.3: Fraction of all masers, megamasers, and disks within the *WISE* AGN selection criteria; detection rates are indicated in parentheses.

Criteria	All Masers	Megamasers	Disks
$W1-W2 \geq 0.8$	28% (20%)	28% (15%)	25% (4.2%)
Jarrett et al. (2011)	26% (16%)	27% (13%)	25% (3.6%)
$W1-W2 \geq 0.5$	45% (16%)	43% (12%)	37% (2.9%)
$W1-W2 < 0.5$	55% (2.9%)	57% (2.3%)	63% (0.8%)

levels of ∼20%, with a significant rise in the expected megamaser and disk detection, which gets boosted by at least a factor of four from the currently low rate of <1%.

Thus, while within the whole population of nearby galaxies there are very few objects with red W1–W2 colors (∼4%; Stern et al. 2012), it is definitely of great value to study these systems carefully, and definitely survey them all for maser emission. However, it is also clear that we will only recover less than a quarter of the whole population of megamasers within this color regime. It is thus of interest to try to understand which other property could be used to distinguish between masers and non-masers within the blue galaxy population as well.

The next section makes an attempt to connect the *WISE* properties of these galaxies with their optical features, and in particular with their optical spectral measurements that provide indications to the degree to which their nuclear are powered by accretion or other sources of energy.

5. Connecting WISE with the Optical Properties of the MCP Galaxies

5.1 Optical Data for the MCP Galaxies

Among the nearby galaxies that reveal emission line activity in their centers, optical constraints to the nature of the dominant ionization power mechanism are provided relatively successfully by emission-line classification diagrams. These diagrams employ line flux ratios to separate radiation from hot, young stars (i.e., H II nuclei) from accretion onto a black hole (i.e., Seyferts, Ss, the AGNs), however, there remains quite a fraction of objects that straddle the borders between these two types: the "transition" (T) objects, and the narrow-lined Low Ionization Nuclear Emission Regions (LINERs, Ls), the nature of which remains ambiguous (e.g., Baldwin, Phillips & Terlevich 1981, Veilleux & Osterbrock 1987, Kewley et al. 2006; Constantin et al. 2015).

Reliable emission-line diagnostic diagram require accurate measurements of the emission-line component after it is separated from the host stellar emission, and subtracted from the total galaxy spectrum. Unfortunately, publicly available optical data of such quality are not widely available. The bulk of the optical spectra are generally acquired for the purpose of measuring redshifts, and they do not necessarily care for flux calibration.

Luckily, wide sky surveys like the Palomar Survey (Ho, Filippenko & Sargent 2003 and references therein), and the SDSS (e.g., DR7; Abazajian et al. 2009) provide the

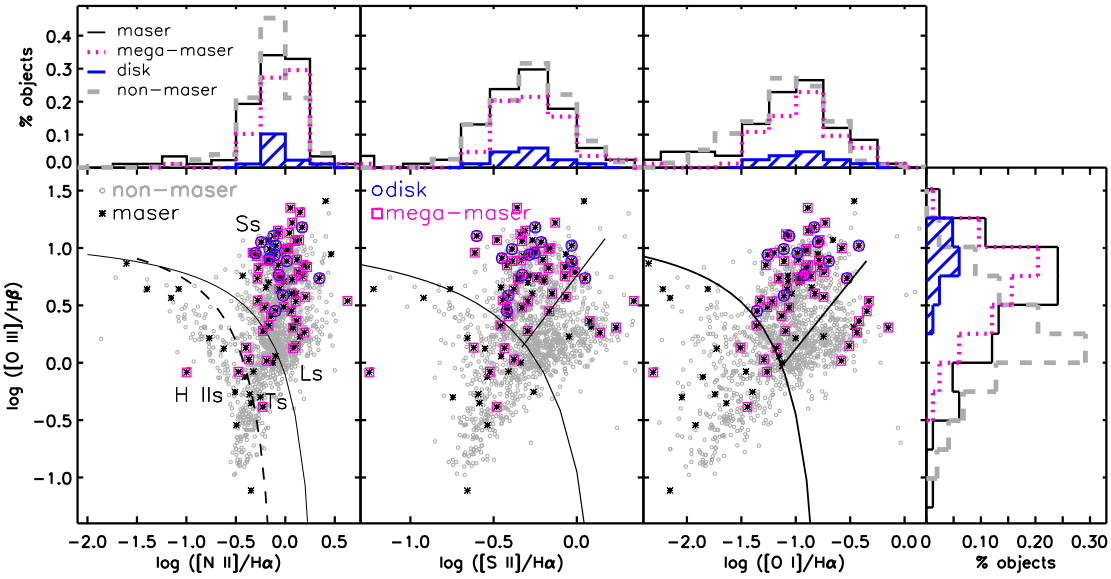

Figure 5.1: Emission-line galaxy classification diagrams for the MCP galaxies with high quality optical spectra. The axes represent emission-line flux ratios, where Hα and Hβ are the first two Hydrogen Balmer lines, [N ii] is the line at λ6583, [S ii] is the sum of the flux emitted at $\lambda\lambda$6716, 6731, and [O i] is the λ6300 feature. Also shown here are the distributions of all line flux ratios for all non-masers and subgroups of masers. The lines in the bottom panels are semi-empirical fits to the distributions of objects in these diagrams.

desired spectral measurements; the nuclear nebular emission of the SDSS galaxies are drawn from the catalog built by the MPA/JHU collaboration[1]. However, a careful cross-matching of the MCP-*WISE* galaxies with these datasets return line flux ratios for only 71 maser galaxies, among which 48 are megamasers. Additional literature search provided optical line flux ratios for nine more maser galaxies, with five of these being megamasers. For the non-masers, we have found 1340 objects with accurate flux measurements. Thus, we can perform optical classifications for only $\sim$ 60% of the MCP-*WISE* sample. Figure 5.1 shows the diagnostic diagram for all these maser and control galaxies, with a comparison of histograms of the involved line ratios, and Table 5.1 lists the proportions in which non-masers and the various types of masers span each spectral type.

[1]Publicly available at http://wwwmpa.mpa-garching.mpg.de/SDSS/ ; (Brinchmann et al. 2004)

Table 5.1: Fractions of optical spectral type per each maser and non-maser sample (each line adds up to 100%). The numbers in parentheses indicate the total number of objects in each sample.

	H II	Transition	Seyfert	LINER
Masers (80)	16%	10%	61%	13%
Megamasers (54)	1.9%	7.4%	76%	15%
Disks (12)	0%	0%	92%	8.3%
Non-Masers (1340)	17%	26%	26%	31%

Interestingly, the optical data suggest that the maser detection rate among Seyferts is high ($\sim$ 8%), however, it is unclear whether this is because the disk-maser emission is genuinely connected to this type of nuclear activity (i.e., the BH accretion process) or is simply a consequence of the same survey bias; the maser surveys targeted almost exclusively type 2 Seyferts. Also, the megamaser disks have only been found among the Seyferts, however, megamasers appear to cover the whole spectral spectrum. The maser fraction is clearly non-zero for non-AGN types, in fact, there is an equal probability to find masers among Ts as in Ls ($\sim$ 10-13%), and even more likely to find them in H IIs ($\sim$ 16%). For some of these, the maser luminosity is only a smidgen below $10L_{\odot}$, leaving them short of being classified as a megamaser, but we have now increasing evidence and reasonable physical explanations for variability (Pesce et al. 2015) that could, in principle, turn these systems into the next disk detection.

Thus, optical data alone is not very useful for connecting the nature of the nuclear power source with the water maser activity.

5.2 Optical Spectral Class and *WISE* Colors for Maser and Non-Maser Galaxies

While the *WISE* color-color diagram proves useful for identifying red (possibly obscured) AGN as an efficient pool of maser galaxies, the *WISE* colors alone are not significantly more successful in finding the bulk of megamaser disk systems. As

we have shown in Section 4.2, of all maser disks, 75% are in fact in the blue (W1–W2 $<$ 0.8) mid-IR region, showing once again that the megamaser disks are not necessarily associated with obscured/reddened Seyfert-type activity, and that the SMBH accretion associated with the maser disk can be, in fact, heavily buried in hosts of other type(s) of dominant emission.

We built here a new *WISE* color-color diagram for all maser and non-maser galaxies, to which we add different symbols to illustrate the optical spectral type, and how this correlates with the *WISE* red colors and color cuts associated with AGN activity. Figure 5.2 shows the WISE (W1–W2, W2–W3) colors and the optical spectral classes of the masers and the non-masers in two separate diagrams.

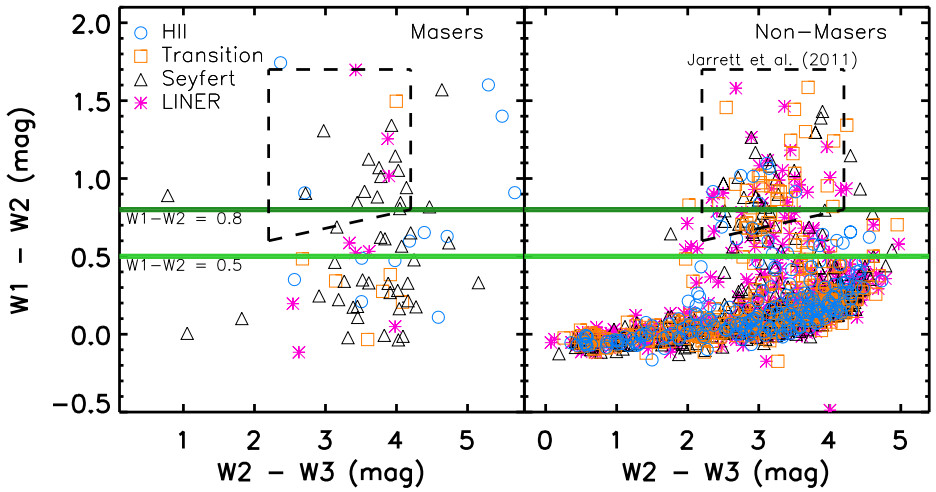

Figure 5.2: The *WISE* (W1–W2, W2–W3) colors of the MCP-*WISE* samples of maser (left panel) and non-maser (right panel) galaxies along with their associated optical spectroscopic class: H II galaxy nuclei (blue circle), Transition galaxies (orange square), Seyferts (black triangle), and LINERS (magenta asterisk). Both panels show the *WISE* red AGN color cuts as described in Section 4.2.

To better explore the relationship between the maser and AGN activities via *WISE* red colors and spectral classifications, we calculated the fraction of objects of a given spectral class that fall into the red/obscured AGN location in the *WISE* color-color cuts presented in Section 4.2. Table 5.2 lists these numbers for the W1–W2 $\geq$ 0.8

cut.

Table 5.2: Fraction of each optical spectral type per each maser and non-maser sample, with *WISE* red colors (W1–W2 $\geq$ 0.8) only. Numbers in parentheses indicate the red sample size and fraction of the total masers, megamasers, disks, and non-masers with optical spectral classification, respectively.

	H II	Transition	Seyfert	LINER
Masers (26, 33%)	38%	13%	35%	30%
Megamasers (18, 33%)	0%	25%	34%	38%
Disks (5, 42%)	0%	0%	45%	0%
Non-Masers (79, 6%)	2.6%	6.9%	6.6%	6.3%

Overall, the fractions of all spectral types of galaxies with red *WISE* colors suggestive of obscured AGNs is higher among masers than among non-masers. While this supports our finding that red *WISE* colors are more prone to revealing maser activity, it also indicates that the red *WISE* galaxies include a non-signifiant fraction of objects that are not classified as AGN based on their optical properties.

Nevertheless, only $\sim$35% of the maser Seyferts have red *WISE* colors suggestive of obscured AGNs, regardless of whether they are defined by the W1–W2 $\geq$ 0.8, the W1–W2 $\geq$ 0.5, or the Jarrett et al. (2011) cuts. There is also a non-negligible fraction (6.6%) of non-maser Seyferts that exhibit red *WISE* colors: i.e., there are red Seyferts that are not associated with any kind of maser emission, and in particular to the powerful megamaser activity; the "seed" radiation (the AGN nucleus, as revealed by the Seyfert class) and the high-column density along the line of sight (as suggested by the red *WISE* colors) appear to both be there, and yet, the maser emission, if existing, is not powerful enough to be detected. It thus look like that there are additional circumstances that play a role in determining the degree to which a galaxy center is maser ready or active.

On the other hand, it is interesting to see that 55% (or 65%) of the megamaser disks (or of all megamasers) optically classified as Seyferts have blue *WISE* colors.

Thus, for more than half of the disk systems, the masing activity appears to be strong without a clear association with obscuration or with substantial red emission caused by reprocessing of the AGN emission by (large amounts of) surrounding dust. Thus, these findings challenge somewhat the idea that megamaser activity needs to be associated with obscured/reddened Seyfert-type activity. While the megamaser disk detection rate seems indeed to increase when red galaxies are targeted, there will be quite a fraction of them missed in such searches.

5.3 Linking the [O III] and Maser Luminosities with the Mid-IR Emission

Another optical parameter that could shed light on the relationship between nuclear obscuration and masing activity is the [O III]λ5007Å emission-line luminosity. The [O III] luminosity has often been employed as a proxy for the strength of the AGN activity in galaxy centers (e.g., Heckman et al. 2014), and in addition, the intrinsic (i.e., extinction-corrected) [O III] flux (or luminosity) seems to be a good sample selection criterion for maximizing the number of detections in maser searches (the maser detection rate increases at higher intrinsic $L_{[OIII]}$, suggesting higher extinction in galaxies more likely to host maser emission; Zhu et al. 2011, Constantin 2012).

We are now able to add a new dimension to these results, by investigating how the water maser and the [O III] luminosities, as well as the relationship between them, link to the mid-IR properties most suggestive of dust obscuration.

In Figure 5.3, we plot the $\log_{10}L_{H_2O}$ (upper panels) and the $\log_{10}L_{[OIII]}$ (lower panels) against the mid-IR luminosity measured in each of the *WISE* bands for the MCP-*WISE* samples of masers, maser subtypes, and non-masers. Obviously, the upper panels show only the galaxies with maser emission, as there is no L_{H_2O} for the non-maser galaxies; we plot here all of the objects for which an estimate of the maser

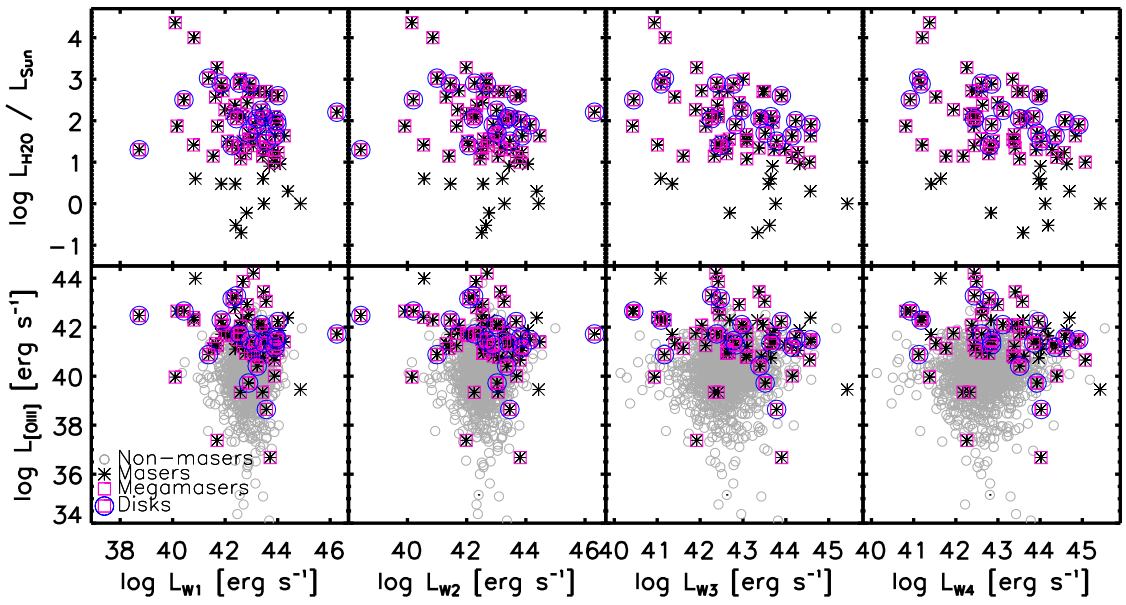

Figure 5.3: Relations between the luminosities in [O III] and water maser emission in all *WISE* bands for the MCP-*WISE* samples. The symbols are as defined in previous figures: all masers (black asterisk), megamasers (magenta square), disks (blue circle around magenta square), and non-masers (gray circle).

luminosity was possible[2], regardless of whether or not there is optical information available for them. The lower panels show only the galaxies (masers and non-masers) with optical classifications discussed in Sections 5.1 and 5.2, as they are the only the objects for which we have reliable measurements of the $L_{[\mathrm{OIII}]}$.

There are some interesting trends seen here: there is a weak negative correlation between the strength of the H_2O maser power and that of the mid-IR wavelengths in all four *WISE* bands, suggesting that stronger mid-IR emission is not necessarily a better indication for powerful maser activity. We also confirm here that the masers clearly favor galaxies with strong [O III] emission. Interestingly, however, among these systems, there seems to be a tendency for stronger [O III] activity where the mid-IR emission is weaker, again, in all of the four *WISE* bands. On the other hand, the

[2]The true luminosity of masers is difficult to measure because the maser emission is likely to be beamed (e.g., Elitzur et al. 1992) and estimates of the beaming angle require a detailed model of the maser, which can only be inferred in the cases with well-understood geometries from VLBI observations (e.g., Miyoshi et al. 1995).

non-masers do not show any trends between the [O III] and the *WISE* emission.

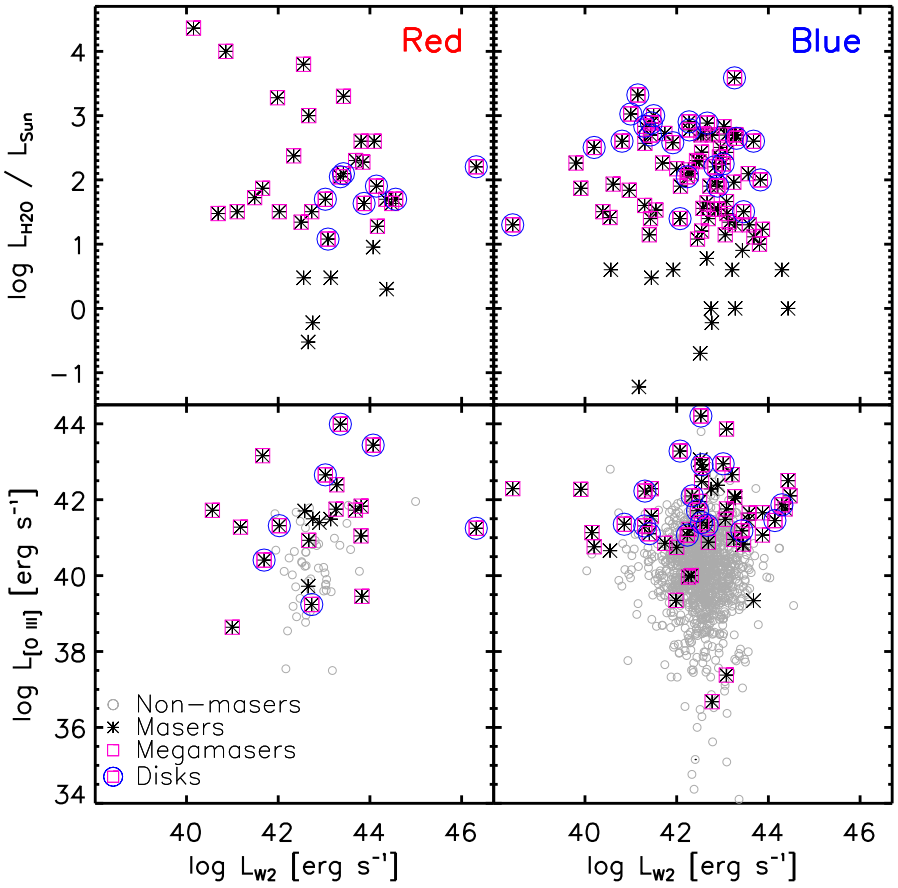

Figure 5.4: H_2O and [O III] luminosities as a function of the W2 luminosity for the MCP-*WISE* maser and non-maser samples with red and *WISE* colors (left and right panels respectively). The red objects are those for which W1–W2 > 0.8, as discussed in Section 4.2.

In an attempt to link these findings to obscuration, we show in Figure 5.4 the relationship between L_{H_2O} and $L_{[OIII]}$ with the *WISE* luminosity, separately for the red and the blue galaxies, defined based on their W1–W2 colors (i.e., W1–W2 ≥ 0.8 for red). We chose to show here only the trends with L_{W2}, however, the conclusions are similar when the other *WISE* bands are considered. These plots show that while the most luminous megamaser emission is found among the red galaxies, it does not have a disk morphology, and is among those galaxies with the lowest L_{W2}. Nevertheless, the red disk megamasers show the strongest mid-IR luminosity. On the other hand,

the blue megamaser disks span the whole spectrum of mid-IR power output exhibited by nearby galaxies, without a clear correlation between these two parameters.

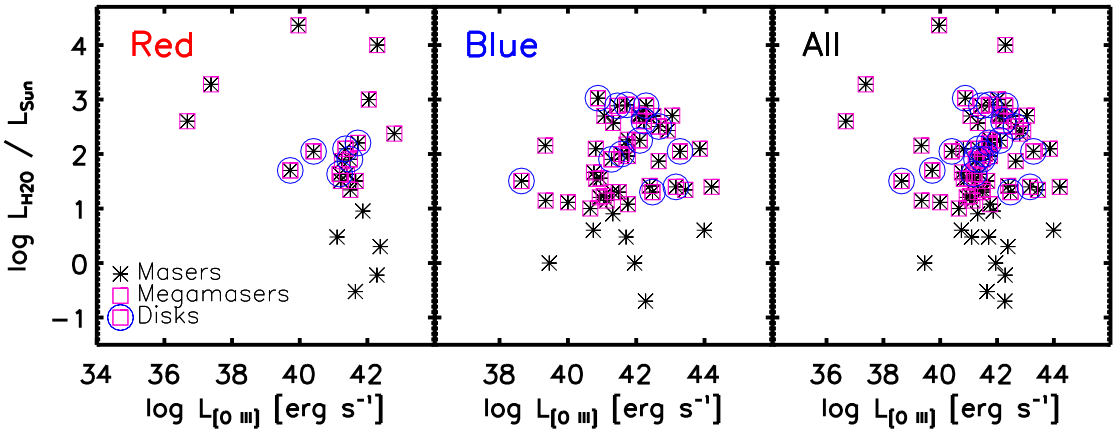

Figure 5.5: Isotropic maser luminosity (L_{H_2O}) versus $L_{[OIII]}$ of all MCP-*WISE* masers and maser subsamples; we show the comparison for the whole sample as well as for the subsamples separated based on their *WISE* blue and red colors.

In Figure 5.5, we show that the relationship between L_{H_2O} and $L_{[OIII]}$ is likely to be different between the red and the blue galaxies. The overall expected trend of stronger maser emission for higher [O III] luminosity which is shown in the far-right panel for the whole sample of maser galaxies with [O III] measurements, is weaker among the red megamaser galaxies; here, the most luminous water maser emission does not exhibit a disk-like configuration.

While the number statistics remain small for this particular type of systems, especially among the megamaser disks, these results support the preference of disk masing systems for higher-extinction that can be explained as a geometrical effect. The idea that we can only observe the megamaser disks when the disks are highly inclined, or close to being edge-on relative to the line of sight, to allow for a long enough length to produce the required amplification, suggests that they should also exhibit strong mid-IR emission (i.e., higher L_{W2} values), and this matches what we have found here: the red water maser emitters with lower L_{W2} do not exhibit disk-like configurations.

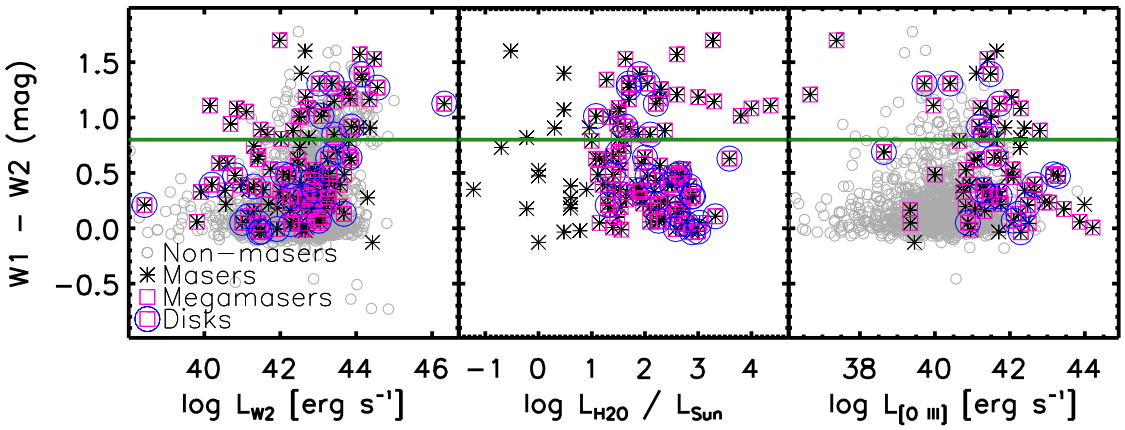

Figure 5.6: *WISE* W1–W2 color versus the luminosity in the W2 band (*left panel*), the isotropic maser luminosity ($L_{\mathrm{H_2O}}$) (*middle panel*), and $L_{[\mathrm{OIII}]}$ (*right panel*) of all MCP-*WISE* masers, maser subsamples, and non-masers. The *WISE* W1–W2 = 0.8 color cut is marked as a green line across each panel to distinguish between the red/dusty AGNs and blue objects.

On the other hand, the washed out trends among the blue megamasers , which do not show any preference for extreme L_{W2}), and whose stronger $L_{\mathrm{H_2O}}$ does not necessarily correlate with higher $L_{[\mathrm{OIII}]}$ pose new challenges. In these systems, it seems that if the AGN strength is readily available for producing the seed maser radiation (high $L_{[\mathrm{OIII}]}$ and Seyfert spectral classification), the line of sight amplification falls short (moderate or minimum of reprocessing by dust, corresponding to moderate or low L_{W2}, and blue mid-IR colors); alternatively, the AGN is weak or dominated by the circumnuclear star-formation (lower $L_{[\mathrm{OIII}]}$), which would fit the blue systems with moderately high $L_{\mathrm{W2}} > 10^{42}$ erg s^{-1}. While among all masers the W1-W2 colors appear redder for higher L_{W2}, the trend disappears when only the blue objects are considered (Figure 5.6). Also W1-W2 do not correlate in any way with either $L_{\mathrm{H_2O}}$ or $L_{[\mathrm{OIII}]}$ luminosities, for either the red or the blue masers. Nevertheless, the intrinsic scatter of these relations are too large to draw statistically significant conclusions from the small samples we can currently employ.

6. Conclusions

Given the rarity of galaxies with water maser emission, and of megamaser disks in particular, as well as the importance for studying them in detail as the most accurate estimation tools for supermassive black holes and cosmological distances, a systematic approach to finding them is essential to increase their number.

Using data from the *Wide-Field Infrared Survey Explorer* (*WISE*), we present here a mid-IR analysis of the properties of the largest sample of galaxies surveyed for H_2O maser emission in 22 GHz, with the goal of better constraining the previously proposed connection between water masing activity and the circumnuclear dust absorption and radiation reprocessing in galaxy centers.

Our main results can be summarized as follows:

- The apparent brightness of the mid-IR emission is relatively useful in separating the masers from the non-masers. The maser detection rates increase considerably, from the mere 3 – 4% recovered by the current surveys, to ∼6%, simply by employing rough cuts in magnitudes. The main gain seems however to apply to the kilomasers, as the megamaser detection rates increase by only ∼30% for all megamasers, and by ∼20% for the megamaser disks specifically. The W3 < 9.9 and W4 < 7.1 magnitudes appear most stringent in selecting masers from non-masers, although contamination by the latter type of galaxies is still significant.

- The mid-IR average colors (<W1-W2>, <W2-W3>, <W3-W4>) of the maser

galaxies are redder than those of the non-masers, and targeting galaxies with colors that fall close to the megamaser average colors ($0.50 <$ W1-W2 < 0.60, $3.43 <$ W2-W3 < 3.55, $2.54 <$ W3-W4 < 2.66) suggests a significant increase in the megamaser detection rate, to a possible 16% detection rate. The disks are redder objects than the non-masers, however, being red is not a defining characteristic of their hosts.

- In an attempt to understand the possible dominant radiation process associated with maser emission, we compared the mid-IR spectral energy distributions (SEDs) of masers and non-masers, and found that the non-maser SEDs remain relatively flat at longer wavelengths while all the maser types rise in intensity, which is consistent with previous trends for redder colors among the masing galaxies. As probably expected, the kilomasers that show the most dramatic change in νL_ν, with the bluest W1-W2 and the reddest W2-W3 colors, which is consistent with emission from hot dusty surroundings of stellar nurseries, as opposed to AGNs.

- On average, the megamasers and their subgroup of disks show total mid-IR luminosities that are intermediate between those of non-masers and the kilomasers, the latter being the most luminous in the wavelength regime probed by *WISE*. The detection rates of megamasers (and of megamaser disks in particular) are highest among the less luminous mid-IR systems ($L_{\rm WISE} < 10^{41}$ erg s^{-1}), showing a possibly huge increase to 15%.

- The mid-IR color cuts for selecting red/dusty AGNs reveal a dramatic increase in the maser detection rates (up to 20% for all masers, 15% for the megamasers, and 4.2% for the disks). Nevertheless, these criteria, which link once again the masing activity with dusty/obscured black hole accretion, would miss the bulk

of the megamaser disks out there: the majority (∼60%) of the masers and disks are found to be hosted by *WISE* blue galaxies.

- When considering the optical properties of the maser and non-maser galaxies in the context of the maser–mid-IR connection, we find that while all maser disk hosts are classified as bona-fide AGNs (i.e., Seyferts) by their optical emission line ratios, only 45% of them fall within the *WISE* color selection criteria for obscured accretion. In an attempt to link the origin of the "seed" radiation for the powerful megamaser emission with the AGN activity, we have investigated the behavior of the [O III] luminosity as a function of various measures of the mid-IR emission, and find no prominent correlations with emission in either of the four *WISE* bands, or the *WISE* colors. While the strength of the water maser emission seems to correlate with the AGN strength (i.e., $L_{[\mathrm{OIII}]}$), it appears more prominent in objects with weaker mid-IR emitting powers, while showing no clear dependence on the *WISE* colors.

In conclusion, although employing mid-IR criteria improves considerably the maser detection rates, the mid-IR emission does not seem to be particularly sensitive or constraining to the maser pumping mechanism. On the other hand, the maser disk detection could remain the only way to acknowledge accreting SMBHs in *WISE* blue hosts whose nuclei do not show clear signs of AGN-like nebular properties, and thus could provide an improved way to compute an improved census of active black holes in galaxy centers.

7. References

Abazajian, K. N., Adelman-McCarthy, J. K., Agüeros, M. A., Allam, S. S., Prieto, C. A., et al. 2009, ApJS, 182:543

Antonucci, R. R. J. & Miller, J. S. 1985, ApJ, 297:621

Ashby, M. L. N., Stern, D., Brodwin, M., Griffith, R., Eisenhardt, P., et al. 2009, ApJ, 701:428

Assef, R. J., Kochanek, C. S., Brodwin, M., Cool, R., Forman, W., et al. 2010, ApJ, 713:970

Assef, R. J., Stern, D., Kochanek, C. S., Blain, A. W., Brodwin, M., et al. 2013, ApJ, 772:26

Baan, W. A., Wood, P. A., & Haschick, A. D. 1982, ApJL, 260:L52

Baldwin, J. A., Phillips, M. M., & Terlevich R. 1981, PASP, 93:5

Bottinelli, L., Fraix-Burnet, D., Gouguenheim, L., Kazes, I., Le Squeren, A. M., et al. 1985, A&A, 151:L7

Braatz, J. A., Wilson, A. S., Henkel, C. 1996a, ApJ, 106:51

Braatz, J. A., Wilson, A. S., Henkel, C. 1997, ApJ, 110:321

Braatz, J. A., Henkel, C., Greenhill, L. J., MOran, J. M., & Wilson, A. S. 2004, ApJ, 617:L29

Braatz, J. A., Reid, M. J., Humphreys, E. M. L., et al. 2010, ApJ, 718:657

Bragg, A. E., Greenhill, L. J., Moran, J. M., & Henkel, C. 2000, ApJ, 535:73

Brinchmann, J., Charlot, S., White, S. D. M., Tremonti, C., Kauffmann, G., et al. 2004, MNRAS, 351:1151

Castangia, P., Panessa, F., Henkel, C., Kadler, M., & Tarchi, A. 2013, MNRAS, 436:3388

Cheung, A. C., Rank, D. M., Townes, C. H., Thornton, D. D., & Welch, W. J. 1969, Nature, 221:626

Churchwell, E., Witzel, A., Huchtmeier, W., Pauliny-toth, I., Roland, J., & Wieber, W. 1977, A&A, 54:969

Claussen, M. J., Heiligman, G. M., & Lo, K. Y. 1984, Nature, 310:298

Claussen, M. J. & Lo, K. Y. 1986, ApJ, 308:592

Claussen, M. J., Reid, M. J., Schneps, M. H., Lo, K. Y., Moran, J. M., Gusten, R. 1988, IAU Symp. 129: The Impact of VLBI on Astrophysics and Geophysics, 129:231

Constantin, A., Green, P., Aldcroft, T., Kim, D. W., Haggard, D., et al. 2009, ApJ, 705:1336

Constantin, A. 2012, JPCS, 372

Constantin, A., Shields, J. C., Ho, L. C., Barth, A. J., Filippenko, A. V., et al. 2015, ApJ, 814:149

Dos Santos, P. M. & Lepine, J. R, D. 1979, Nature, 278:34

Elitzur, M., Hollenbach, D. J., & McKee, C. F. 1992, ApJ, 394:221

Elmegreen, B. G. & Morris, M. 1979, ApJ, 229:593

Filippenko, A. V. & Sargent, W. L., W. 1985, ApJS, 57:503

Gao, F., Braatz, J. A., Reid, M. J., et al. 2016, ApJ, 817:128

Genzel, R. & Downes, D. 1977, ARA&A, 30:145

Greenhill, L. J., Henkel, C., Becker, R., Wilson, T. L., Wouterloot, J. G. A. 1995a, A&A, 304:21

Greenhill, L. J., Jiang, D. R., Moran, J. M., Reid, M. J., Lo, K. Y., Claussen, M. J. 1995b, ApJ, 440:619

Greenhill, L. J., Tilak, A., & Madejski, G. 2008, ApJ, 686:L13

Gundermann, E. 1965. PhD Thesis. Harvard Univ. Cambridge, Mass.

Haschick, A., Baan, W., & Peng, E. W. 1994, ApJ, 437:L35

Heckman, T. M. & Best, P. N. 2014, ARA&A, 52:589

Herrnstein, J. R., Moran, J. M., Greenhill, L. J., Diamond, P. J., Inoue, M., et al. 1999, Nature, 400:539-541

Herrnstein, J. R., Moran, J. M., Greenhill, L. J., & Trotter, A. S. 2005, ApJ, 629, 719

Ho, L. C., Filippenko, A. V., & Sargent, W. L. W. 2003, ApJ, 583:159

Hu, W. 2005, ASP Conference Series, 339

Humphreys, E. M. L., Reid, M. J., Moran, J. M., Greenhill, L. J., & Argon, A. L. 2013, ApJ, 775:13

Impellizzeri, C. M. V., McKean, J. P., Castangia, P., Roy, A. L., Henkel, C., et al. 2008, Nature, 456:927

Jarrett, T., Cohen, M., Masci, F., et al. 2011, ApJ, 735:112

Kewley, L. J., Groves, B., Kauffmann, G., & Heckman, T. 2006, MNRAS, 372:961

Kondratko, P. T., Greenhill, L. J., & Moran, J. M. 2006, ApJ, 652:136

Kuo, C. Y., Braatz, J. A., Condon, J. J., et al. 2011, ApJ, 727:20

Kuo, C. Y., Braatz, J. A., Redi, M. J., et al. 2013, ApJ, 767:155

Kuo, C. Y., Braatz, J. A., Lo, K. Y., et al. 2015, ApJ, 800:26

Liu, Z. W., Zhang, J. S., Henkel, C., Liu, J., Müller, P., et al. 2017, MNRAS, 466:1608

Lo, K. Y. 2005, ARA&A, 43:625

Lynden-Bell, D. 1969, Nature, 223:690

Maoz, E. 1995, ApJL, 455:L131

Merloni, A. 2015, in Haardt F., *Lecture Notes in Physics, Vol. 905, Astrophysical Black Holes*, Springer, Switzerland, 101

Miyoshi, M., Moran, J. M., Herrnstein, J., Greenhill, L., Nakai, N., et al. 1995, Nature, 373:127

Moran, J. M., Greenhill, L. J., Herrnstein, J., Diamond, P., Miyoshi, M., et al. 1995, Proc. Natl. Acad. Sci., USA 92:11427

Nakai, N., Inoue, M., Miyoshi, M. 1993, Nature, 361:45

Netzer, H. 2015, ARA&A, 53:365

Olling, R. P. 2007, MNRAS, 378:1385

Ott, J., Meier, D. S., McCoy, M., Peck, A., Impellizzeri, V., et al. 2013, ApJ, 771:L41

Palagi, F., Cesaroni, R., Comoretto, G., Felli, M., & Natale, V. 1993, A&AS, 101:153

Pesce, D. W., Braatz, J. A., Condon, J. J., Gao, F., Henkel, C., et al. 2015, ApJ, 810:65

Ramolla, M., Haas, M., Bennert, V. N., & Chini, R. 2011, A&A, 530:A147

Reid, M. J., Braatz, J. A., Condon, J. J., et al. 2009, ApJ, 695:287

Reid, M. J. 2012, IAU Symp. 287: Maser Astrometry: from Galactic Structure to Local Group Cosmology, 287:359

Reid, M. J., Braatz, J. A., Condon, J. J., et al. 2013, ApJ, 767:154

Salpeter, E. E. 1964, ApJ, 140:796

Sanders, D. B. & Mirabel I. F. 1996, ARA&A, 34:749

Satyapal, S., Secrest, N. J., McAlpine, W., et al. 2014, ApJ, 784:113

Stern, D., Assef, R. J., Benford, D. J., et al. 2012, ApJ, 753:30

Van den Bosch, R. C. E., Greene, J. E., Braatz, J. A., Constantin, A., & Kuo C. Y. 2016, ApJ, 819:11

Veilleux, S. & Osterbrock, D. E. 1987, ApJS, 63:295

Walker, R. C., Matsakis, D. N., & Garcia-Barreto, J. A. 1982, ApJ, 255:128

Weaver, H., Williams, D. R. W., Dieter, N. H., & Lum, W. T. 1965, Nature, 208:29

Wright, E. L., Eisenhardt, P. R. M., Mainzer, A. M., Ressler, M. E., et al. 2010, ApJ,

140:1868

Zhang, J. S., Henkel, C., Kadler, M., Greenhill, L. J., Nagar, N., et al. 2006, A&A, 450:933

Zhang, J. S., Henkel, C., Guo, Q., Wang, H. G., & Fan, J. H. 2010, ApJ, 708:1528

Zhang, J. S., Henkel, C., Guo, Q., & Wang, J. 2012, A&A, 538:A152

Zhu, G., Zaw, I., Blanton, M. R., & Greenhill, L. J. 2011, ApJ, 742:73